

Chapter 12

Artificial Neural Network Based Methodologies for the Estimation of Wind Speed

Despina Deligiorgi, Kostas Philippopoulos
and Georgios Kouroupetroglou

Abstract Recent advances in artificial neural networks (ANN) propose an alternative promising methodological approach to the problem of time series assessment as well as point spatial interpolation of irregularly and gridded data. In the field of wind power sustainable energy systems ANNs can be used as function approximators to estimate both the time and spatial wind speed distributions based on observational data. The first part of this work reviews the theoretical background, the mathematical formulation, the relative advantages, and limitations of ANN methodologies applicable to the field of wind speed time series and spatial modeling. The second part focuses on implementation issues and on evaluating the accuracy of the aforementioned methodologies using a set of metrics in the case of a specific region with complex terrain. A number of alternative feedforward ANN topologies have been applied in order to assess the spatial and time series wind speed prediction capabilities in different time scales. For the temporal forecasting of wind speed ANNs were trained using the Levenberg–Marquardt backpropagation algorithm with the optimum architecture being the one that minimizes the Mean Absolute Error on the validation set. For the spatial estimation of wind speed the nonlinear Radial basis function Artificial Neural Networks are compared versus the linear Multiple Linear Regression scheme.

D. Deligiorgi (✉)

Department of Physics Division of Environmental Physics and Meteorology,
University of Athens, Panepistimioupolis, Ilisia 15784 Athens, Greece
e-mail: despo@phys.uoa.gr

G. Kouroupetroglou

Department of Informatics and Telecommunications, Division of Signal Processing and
Communication, University of Athens, Panepistimioupolis, Ilisia 15784 Athens, Greece
e-mail: koupe@di.uoa.gr

K. Philippopoulos

Division of Environmental Physics-Meteorology, Department of Physics, University of
Athens, Panepistimioupolis, Ilisia 15784 Athens, Greece

12.1 Introduction

During the past few decades, there has been a substantial increase in the interest on artificial neural networks (ANN). ANNs have been successfully adopted in solving complex problems in many fields. Essentially, ANNs provide a methodological approach in solving various types of nonlinear problems that are difficult to deal with using traditional techniques. Often, a geophysical phenomenon exhibits temporal and spatial variability, and is suffering by issues of nonlinearity, conflicting spatial and temporal scale, and uncertainty in parameter estimation (Deligiorgi and Philippopoulos 2011). ANNs have been proved to be flexible models that have the capability to learn the underlying relationships between the inputs and outputs of a process, without needing the explicit knowledge of how these variables are related. Kalogirou presented a detailed review of the application of ANN in a variety of renewable energy systems (Kalogirou 2001).

Wind power renewable energy generation is growing rapidly in the past two decades. The accurate forecasting of wind speed is critical for wind power generation in order to reduce the reserve capacity and to increase the wind power penetration (Lei et al. 2009). One can find a review on the history of wind speed short-term prediction for wind power generation (Costa et al. 2008). Traditional spatial interpolation methods have been used to estimate wind speed at unsampled locations, using point observations within the same region under study. Cellura et al. have employed the Inverse distance weighted method and the Kriging geostatistical approach to produce wind speed maps for the island of Sicily (Cellura et al. 2008). Furthermore, Luo et al. compared seven spatial interpolation methodologies in order to determine their suitability for estimating daily mean wind speed surfaces in England and Wales and found that the cokriging scheme was most likely to produce the best estimation of a continuous wind speed surface (Luo et al. 2008). In the field of wind speed prediction, conventional time series models have been widely employed to generate short-term wind speed predictions (Cadenas and Rivera 2007; Kamal and Jafri 1997; Poggi et al. 2003). Torres et al. (2005) utilized ARMA models for forecasting wind speed up to 10 h in advance in Navarre, Spain and found that they outperform the persistence model especially in the longer term forecasts.

A classification of the various methods with different time scales for the estimation of wind speed has been presented recently (Soman et al. 2010). Among them, ANNs are characterized as an accurate approach for the short-term (i.e., 30 min–6 h ahead) prediction and their hybrid structures useful for the medium to long-term forecasts. Beyer et al. (1994) used an ANN with a rather simple topology for wind speed prediction, while more complex ANN structures did not improve the results further. Kariniotakis et al. developed a recurrent high order ANN for the prediction of the power output profile of a wind park (Kariniotakis 1996). Mohandes et al. (1998) applied an ANN for wind speed prediction and compared its performance with an autoregressive model for the area of Jeddah, Saudi Arabia. More and Deo (2003) used both Feed Forward as well as recurrent

ANNs to forecast daily, weekly as well as monthly wind speeds at two coastal locations in India. Barbounis and Theocharis used local recurrent ANNs with on-line learning algorithms, based on the recursive prediction error, for the wind speed prediction in wind farms (Barbounis and Theocharis 2007). Li and Shi presented a comparative study on the application of three typical ANN in one-hour-ahead wind speed forecasting for two sites in North Dakota (Li and Shi 2010). Fadare used ANNs to produce monthly maps for the assessment of wind energy potential for different locations within Nigeria (Fadare 2010). In order to improve the performance of the wind speed prediction process, Bouzgou, and Benoudjit proposed a multiple architecture system that combines ANNs, Multiple Linear Regression (MLR), and Support Vector Machines (Bouzgou and Benoudjit 2011). Finally, Philippopoulos and Deligiorgi assess the spatial predictive ability of ANNs to estimate mean hourly wind speed values in a region with complex topography and compare the results with five traditional spatial interpolation schemes (Philippopoulos and Deligiorgi 2012). Moreover, in their work the effect of the inclusion of wind direction is assessed and the ANNs are examined for their capacity to incorporate the mean wind characteristics in the study area.

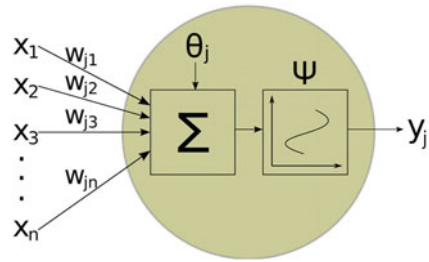
An important aspect of a wind resource assessment program is the wind resource evaluation, which relies heavily on the quality and the availability of wind speed data. A common approach to overcome the problem of limited on-site data availability is the measure–correlate–predict (MCP) method, which makes use of the long-term wind data from nearby climatological stations and a short-term wind speed record from the site under study. The method, based on various correlation techniques, employs the statistical relationship between the two wind speed time series. Under this framework, ANNs have been used as a nonlinear MCP model (Oztopal 2006; Bilgili et al. 2007) and are found, compared to linear MCP algorithms, to decrease significantly the associated wind speed estimation error (Velázquez et al. 2011).

In this work first we review the theoretical background, the mathematical formulation, the relative advantages, and limitations of ANN methodologies applicable to the field of wind speed time series and spatial modeling. In the second part we focus on implementation issues and on evaluating the accuracy of the aforementioned methodologies using a set of metrics in the case of a specific region with complex terrain at Chania, Crete Island, Greece. A number of alternative feedforward ANN topologies are applied in order to assess the spatial and time series wind speed prediction capabilities in different time scales.

12.2 Artificial Neural Networks

Artificial neurons are process element (PE) that attempt to simulate in a simplistic way the structure and function of the real physical biological neurons. A PE in its basic form can be modeled as nonlinear element (see Fig. 12.1) that first sums its weighted inputs $x_1, x_2, x_3, \dots, x_n$ (coming either from original data, or from the

Fig. 12.1 Functional model of an artificial neuron or process element (PE)



output of other neurons in a neural network) and then passes the result through an activation function Ψ (or transfer function) according to the formula:

$$y_i = \Psi \left(\sum_{i=1}^n x_i w_{ji} + \theta_j \right) \tag{12.1}$$

where y_j is the output of the artificial neuron, θ_j is an external threshold (or bias value) and w_{ji} are the weight of the respective input x_i which determines the strength of the connection from the previous PE's to the corresponding input of the current PE. Depending on the application, various nonlinear or linear activation functions Ψ have been introduced (Fausett 1994; Bishop 1995) like the: signum function (or hard limiter), sigmoid limiter, quadratic function, saturation limiter, absolute value function, Gaussian and hyperbolic tangent functions (Fig. 12.2). ANN are signal or information processing systems constituted by an assembly of a large number of simple Processing Elements, as they have been described above. The PE of a ANN are interconnected by direct links called connections and cooperate to perform a Parallel Distributed Processing in order to solve a specific computational task, such as pattern classification, function approximation, clustering (or categorization), prediction (or forecasting or estimation), optimization, and control. One of the main strength of ANNs is their capability to adapt themselves by modifying the interaction between their PE. Another important feature of ANNs is their ability to automatically learn from a given set of representative examples.

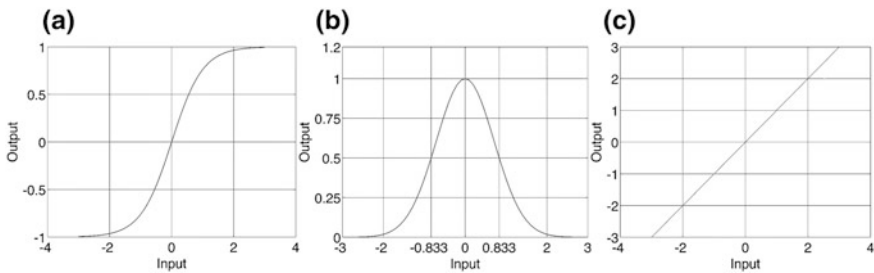


Fig. 12.2 Examples of activation functions Ψ : **a** hyperbolic tangent sigmoid transfer function, **b** Gaussian: $\text{radbas}(n) = \exp(-n^2)$ and **c** linear

The architectures of ANNs can be classified into two main topologies: (a) Feedforward multilayer networks (FF-ANN) in which feedback connections are not allowed and (b) Feedback recurrent networks (FB-ANN) in which loops exist. FF-ANNs are characterized mainly as static and memory-less systems that usually produce a response to an input quickly (Jain et al. 1996). Most FF-ANNs can be trained using a wide variety of efficient conventional numerical methods. FB-ANNs are dynamic systems. In some of them, each time an input is presented, the ANN must iterate for a potentially long time before it produces a response. Usually, they are more difficult to train FB-ANNs compared to FF-ANNs.

FF-ANNs have been found to be very effective and powerful in prediction, forecasting or estimation problems (Zhang et al. 1998). Multilayer perceptrons (MLPs) (Fig. 12.3) and Radial basis function (RBF) topologies (Fig. 12.4) are the two most commonly used types of FF-ANNs. Essentially, their main difference is the way in which the hidden PEs combine values coming from preceding layers: MLPs use inner products, while RBF constitutes a multidimensional function which depends on the distance $r = \|x - c\|$ between the input vector x and the center c (where $\|\cdot\|$ denotes a vector norm) (Powell 1987). As a consequence, the training approaches between MLPs and RBF-based FF-ANN is not the same, although most training methods for MLPs can also be applied to RBF ANNs. In RBF FF-ANNs the connections of the hidden layer are not weighted and the hidden nodes are PEs with a RBF, however, the output layer performs simple weighted summation of its inputs, like in the case of MLPs. One simple approach to approximate a nonlinear function is to represent it as a linear combination of a number of fixed nonlinear RBFs $\{z_i(x)\}$, according to:

$$\Phi(x) = \sum_{i=1}^l z_i(x)w_i \tag{12.2}$$

Fig. 12.3 Multilayer perceptron Feedforward ANN network architecture

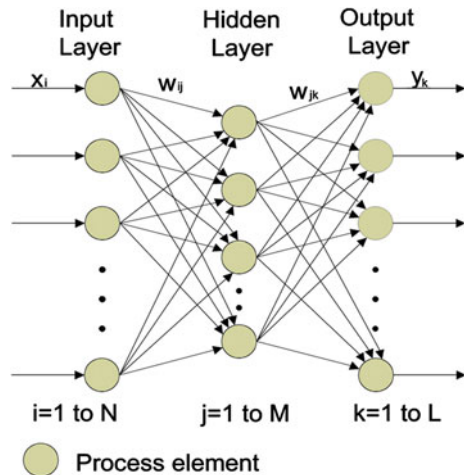
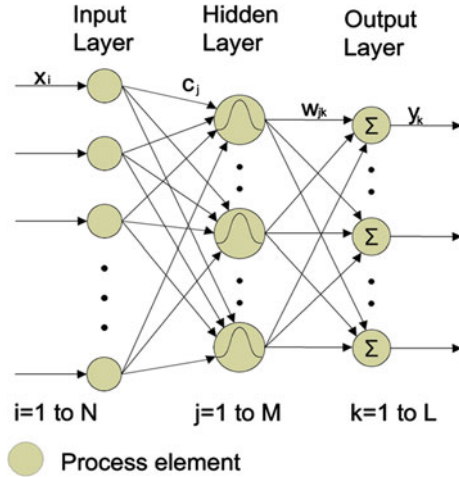


Fig. 12.4 Radial basis function FF-ANN architecture



Typical choices for RBFs $z_i = F(\|x - c\|)$ are: piecewise linear approximations, Gaussian function, cubic approximation, multiquadratic function, and thin plate splines.

A MLP FF-ANN can have more than one hidden layer. But theoretical research has shown that a single hidden layer is sufficient in that kind of topologies to approximate any complex nonlinear function (Cybenko 1989; Hornik et al. 1989).

There are two main learning approaches in ANNs: (1) supervised, in which the correct results are known and they are provided to the network during the training process, so that the weights of the PEs are adjusted in order its output match the target values and (2) unsupervised, in which the ANN performs a kind of data compression, looking for correlation patterns between them and by applying clustering approaches. Moreover, hybrid learning (i.e., a combination of the supervised and unsupervised methodologies) has been applied in ANNs. Numerous learning algorithms have been introduced for the above learning approaches (Jain et al. 1996).

The introduction of the back propagation learning algorithm (Rumelhart et al. 1986) to obtain the weight of a multilayer MLP could be regarded as one of the most significant breakthroughs for training ANNs. The objective of the training is to minimize the training mean square error E_{mse} of the ANN output compared to the required output for all the training patterns:

$$E_{mse} = \sum_{k=1}^p E_k = \frac{1}{2N} \sum_{j=Y} \sum_{k=1}^p (y_i - d_{kj})^2 \tag{12.3}$$

where: E_k is the partial network error, p is the number of the available patterns and Y the set of the output PEs. The new configuration in time $t > 0$ is calculated as follows:

$$w_{ji}(k) = w_{ji}(k-1) - \alpha \frac{\partial E}{\partial w_{ji}} + \beta [w_{ji}(k-1) - w_{ji}(k-2)] \quad (12.4)$$

where $0 < \alpha < 1$ is the speed of learning, β is the momentum and the constant α determines the speed of the training. If a low α value is set, the network weights react very slowly. On the contrary, high α values cause divergence, i.e., the algorithm fails. Therefore, the parameter α is set experimentally.

To speed up the training process, the faster Levenberg–Marquardt Back propagation Algorithm has been introduced (Yu and Wilamowski 2011). It is fast and has stable convergence and it is suitable for training ANN in small- and medium-sized problems. The new configuration of the weights in the $k + 1$ step is calculated as follows:

$$w(k+1) = w(k) - (J^T J + \lambda I)^{-1} J^T \varepsilon(k) \quad (12.5)$$

The Jacobian matrix for a single PS can be written as follows:

$$J = \begin{bmatrix} \frac{\partial \varepsilon_1}{\partial w_1} & \cdots & \frac{\partial \varepsilon_1}{\partial w_n} & \frac{\partial \varepsilon_1}{\partial w_0} \\ \vdots & & \vdots & \vdots \\ \frac{\partial \varepsilon_p}{\partial w_1} & \cdots & \frac{\partial \varepsilon_p}{\partial w_n} & \frac{\partial \varepsilon_p}{\partial w_0} \end{bmatrix} = \begin{bmatrix} x_{1_1} & \cdots & x_{n_1} & 1 \\ \vdots & & \vdots & \vdots \\ x_{1_p} & \cdots & x_{n_p} & 1 \end{bmatrix} \quad (12.6)$$

where: w is the vector of the weights, w_0 is the bias of the PE and ε is the error vector, i.e., the difference between the actual and the required value of the ANN output for the individual pattern. The parameter λ is modified based on the development of the error function E .

12.3 Application of ANN in Wind Speed Estimation

The present work aims to quantify the ability of ANNs to estimate and model the temporal and spatial wind speed variability at a coastal environment. We focus on implementation issues and on evaluating the accuracy of the aforementioned methodologies in the case of a specific region with complex terrain. A number of alternative ANN topologies are applied in order to assess the spatial and time series wind speed prediction capabilities in different time scales.

Moreover, this work presents an attempt to develop an extensive model performance evaluation procedure for the estimation of the wind speed using ANNs. This procedure incorporates a variety of correlation and difference statistical measures. In detail, the correlation coefficient (R), the coefficient of determination (R^2), the mean bias error (MBE), the mean absolute error (MAE), the root mean square error (RMSE), and the index of agreement (d) are calculated for the examined predictive schemes. The formulation and the applicability of such measures are extensively reported in (Fox 1981; Willmott 1982; Willmott et al. 1985).

12.3.1 Area of Study and Experimental Data

The study area is the Chania plain, located on the northwestern part of the island of Crete in Greece. The greater area is constricted by physical boundaries, which are the White Mountains on the south, the Aegean coastline on the northern and eastern part, and the Akrotiri peninsula at the northeast of Chania city (Fig. 12.5). The topography of the region is complex due to the geophysical features of the region. The influence of the island of Crete on the wind field, especially during summer months and days where northerly etesian winds prevail, is proven to cause a leftward deflection and an upstream deceleration of the wind vector (Koletsis et al. 2009, 2010; Kotroni et al. 2001). Moreover, the wind direction of the local field at the broader area of Chania city varies significantly due to the different topographical features (Deligiorgi et al. 2007).

In this study, mean hourly wind speed and direction data are obtained from a network of six meteorological stations, namely TEI, Souda, Platanias, Malaxa, Pedio Volis, and Airport (Fig. 12.5). The measurement sites cover the topographical and land-use variability of the region (Table 12.1). TEI, Souda, and Malaxa stations are situated along the north–south axis, perpendicular to the Aegean coastline. Moreover, TEI and Platanias stations are representative of the coastal character of the region and the climatological station at the Airport of the meteorological conditions that prevail at the Akrotiri peninsula. TEI station is located at the east and in close proximity to the densely populated urban district of Chania city and in this application it will be used as the reference station for examining the performance of the temporal and spatial ANN models. Its wind speed characteristics are presented in Fig. 12.6 in terms of the resulting wind rose

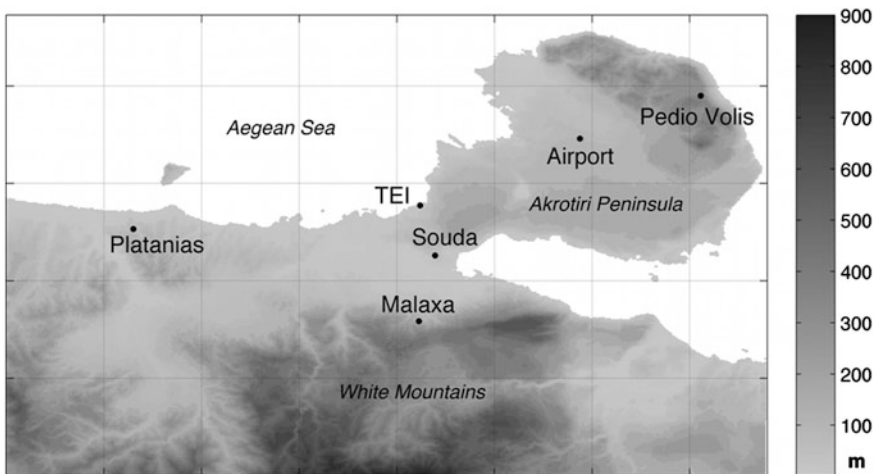


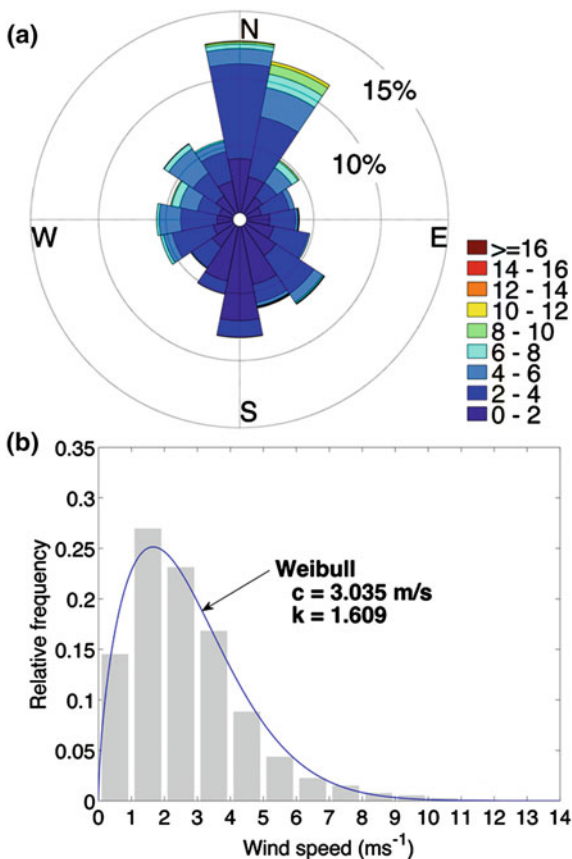
Fig. 12.5 Area of study and location of meteorological stations

Table 12.1 Geographical characteristics of the meteorological stations

	Latitude (°N)	Longitude (°W)	Elevation (m)	Characterization
TEI	35°31'09''	24°02'33''	38	Suburban–Coastal
Souda	35°30'30''	23°54'40''	118	Suburban
Platanias	35°29'46''	24°03'00''	23	Rural–Coastal
Malaxa	35°27'57''	24°02'33''	556	Rural
Pedio Volis	35°34'11''	24°10'20''	422	Rural

diagram (Fig. 12.6a), the wind speed distribution for the overall experimental period along with the corresponding Weibull distribution fit (Fig. 12.6b). The mean wind speed is 2.706 ms^{-1} and the higher wind speed values are associated with northern to northeastern flows during the cold and the transitional (spring and autumn) periods of the year, as a consequence of the combined effect of the synoptic, regional, and small-scale systems.

Fig. 12.6 Wind speed characteristics for the meteorological station TEI



12.3.2 Temporal Forecasting of Wind Speed

12.3.2.1 ANN Implementation Methodology

For the temporal forecasting of wind speed, ANNs are used as function approximators aiming to estimate the wind speed in a location using the current and previous wind speed observations from the same site.

In this application the FeedForward Neural Network architecture with one hidden layer is selected for predicting the wind speed time series. The wind speed characteristics (rose diagrams and wind speed frequency distributions) for the meteorological station of TEI are presented in Fig. 12.6.

Separate ANNs are trained and tested for predicting the 1 h (ANN_T1), 2 h (ANN_T2), and 3 h (ANN_T3) ahead wind speed at TEI, based on the current and the five previous wind speed observations from the same site. Therefore, the input in each ANN is the wind speed at t , $t - 1$, $t - 2$, $t - 3$, $t - 4$, and $t - 5$ and the output is the wind speed at: $t + 1$ for the ANN_T1, $t + 2$ for the ANN_T2, and $t + 3$ for the ANN_T3.

The study period is from August 2004 to September 2006 and due to missing observations the input datasets consist of 11,607 samples of six consecutive hourly observations for the ANN_T1 model, 11,537 and 11,540 six-element vectors for the ANN_T2, and ANN_T3 models, respectively. In all cases, the first 60 % of the dataset is used for training the ANNs, the subsequent 20 % for validation and the remaining 20 % for testing.

The optimum architecture (number of PEs in the hidden layer) is related to the complexity of the input and output mapping, along with the amount of noise and the size of the training data. A small number of PEs result to a non-optimum estimation of the input–output relationship, while too many PEs result to overfitting and failure to generalize (Gardner and Dorling 1998). In this study the selection of the number of PEs in the hidden layer is based on a trial and error procedure and the performance is measured using the validation set. In each case, ANNs with a varying number from 5 to 25 PEs in the hidden layer were trained using the Levenberg–Marquardt backpropagation algorithm with the optimum architecture being the one that minimizes the MAE on the validation set.

The dimensioned evaluations of model-performance error should be based on MAE (Willmott and Matsuura 2005), although the RMSE or the Mean Square Error (MSE) are widely used in the literature. A drawback of the backpropagation algorithm is its sensitivity to initial weights.

During training, the algorithm can become trapped in local minima of the error function, preventing it from finding the optimum solution (Heaton 2005). In this study and for eliminating this weakness, each network is trained multiple times (50 repetitions) with different initial weights. A hyperbolic tangent sigmoid transfer function $\text{tansig}(n) = 2/(1 + \exp(-2n)) - 1$ (Fig. 12.2a) was used as the activation function Ψ for the PEs of the hidden layer. In the output layers, PEs with a linear transfer function were used (Fig. 12.2c).

Table 12.2 Optimum ANN architecture—number of PEs at the input, hidden, and output layer

ANN_T1	ANN_T3	ANN_T2
6-7-1	6-20-1	6-15-1

12.3.2.2 Results

The optimum topologies of the selected ANNs that minimized the MAE on the validation set are presented in Table 12.2. In all cases, the architecture includes six PEs in the input layer and one PE in the output layer. The results indicate that the number of the neurons in the hidden layer is increased as the lag for forecasting the wind speed is increased.

The model evaluation statistics for the TEI station are presented in Table 12.3 and the observed and predicted time series are compared in the scatter plots of Fig. 12.7 and in Fig. 12.8, where a fraction of both time series is illustrated. A general remark is that the ANNs performance is decreased with increasing the forecasting lag. In all cases the MAE is less than 1 ms^{-1} and the explained variance decreases from 79.74 % for the ANN_T1 to 55.98 % for the ANN_T3 model.

The ANN_T1 model exhibits very good performance, as it is observed from the limited dispersion along the optimum agreement line of the 1 h wind speed prediction (Fig. 12.7a). The data dispersion for the ANN_T2 (Fig. 12.7b) and for the ANN_T3 (Fig. 12.7c) scatter plots is increased and a small tendency of over-estimation of the low wind speed values along with an under estimation of the high wind speed values is observed. The effect of this finding in the overall model performance is minimal for the ANN_T2 model (Fig. 12.8b) and becomes relatively important for the 3 h ahead prediction (Fig. 12.8c). Regarding the residuals distributions (Fig. 12.9), the errors for the ANN_T1 and for the ANN_T2 are approximately centered at 0 ms^{-1} , while for the ANN_T3 model the maxima of the distribution is shifted to the left (negative residual values).

12.3.3 Spatial Estimation of Wind Speed

12.3.3.1 ANN Implementation Methodology

For the spatial estimation of wind speed the nonlinear RBF-ANN are compared versus the linear MLR scheme.

Table 12.3 ANN-based model performance

	R	R^2	MBE (ms^{-1})	MAE (ms^{-1})	RMSE (ms^{-1})	d
ANN_T1	0.8930	0.7974	0.0150	0.5942	0.8969	0.9377
ANN_T2	0.8056	0.6490	0.0070	0.8156	1.1801	0.8855
ANN_T3	0.7482	0.5598	-0.0258	0.9494	1.3149	0.8321

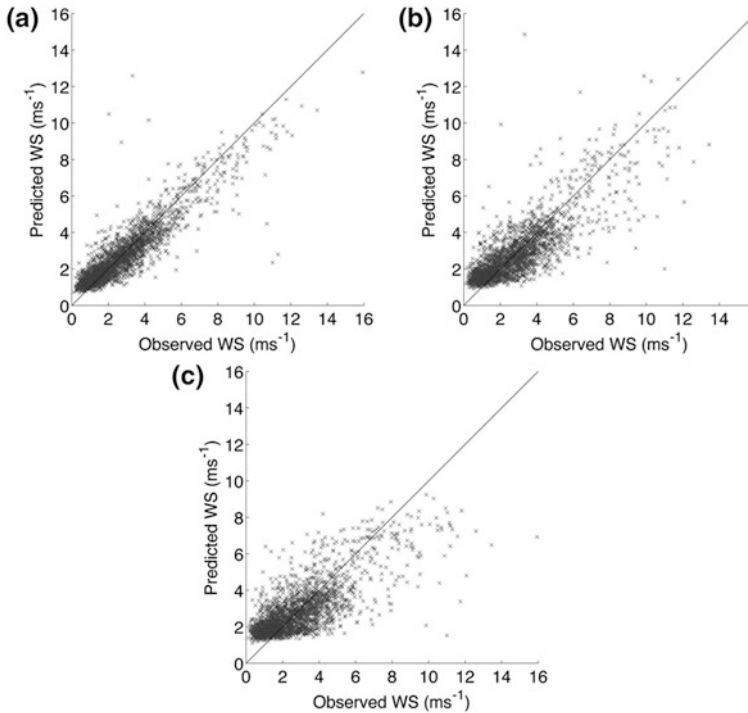


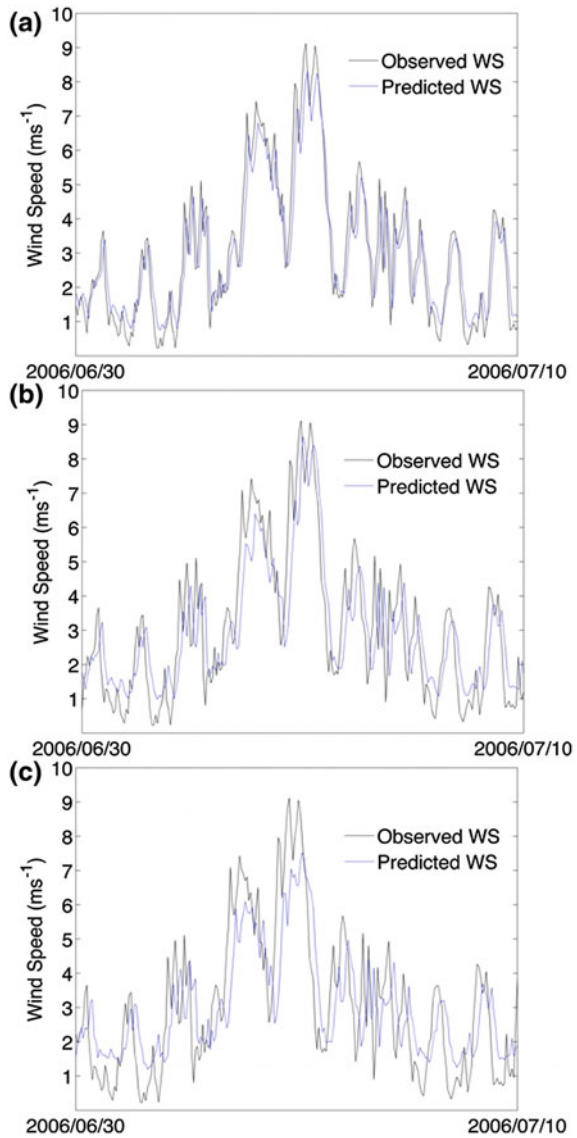
Fig. 12.7 Comparison of the observed and ANN-based predicted wind speed values for $t + 1$ (a), $t + 2$ (b) and $t + 3$ (c)

The target station is located at TEI, while the concurrent wind speed observations from the remaining sites—control stations (Souda, Malaxa, Platanias, PedioVolis, and Airport) are used as inputs in the RBF-ANN model. In an analogous procedure for the MLR scheme, the wind speed at TEI is regarded as the response variable and the wind speed observations at the control stations as the explanatory variables.

The 60 % of the available data (7,300 cases) was used for building and training the models (training set), the subsequent 20 % as the validation set and the remaining 20 % (2433 cases from 2006/01/24 to 2006/08/31) as the test set which is used to examine the performance of both the RBF-ANN and the MLR models. In the case of the RBF-ANN, the validation set is used for selecting the optimum value of the spread parameter, using the trial and calculating the error procedure by minimizing the MAE.

The ANN used had five inputs, a hidden layer with radial basis with 7,300 artificial neurons with Gaussian activation functions $\text{radbas}(n) = \exp(-n^2)$ (Fig. 12.2b) and the output layer has one PE with linear activation function (Fig. 12.2c).

Fig. 12.8 Time series comparison from 2006/06/30 to 2006/07/10 for $t + 1$ (a), $t + 2$ (b) and $t + 3$ (c)



12.3.3.2 Results

The parameters of the MLR equation calculated from the experimental data were:

$$\begin{aligned}
 WS_{TEI} = & -0.2031 + 0.3762WS_{SOU} + 0.4064WS_{PLA} \\
 & + 0.0318WS_{MAL} + 0.0577WS_{PBK} + 0.0370WS_{AIR}
 \end{aligned}
 \tag{12.7}$$

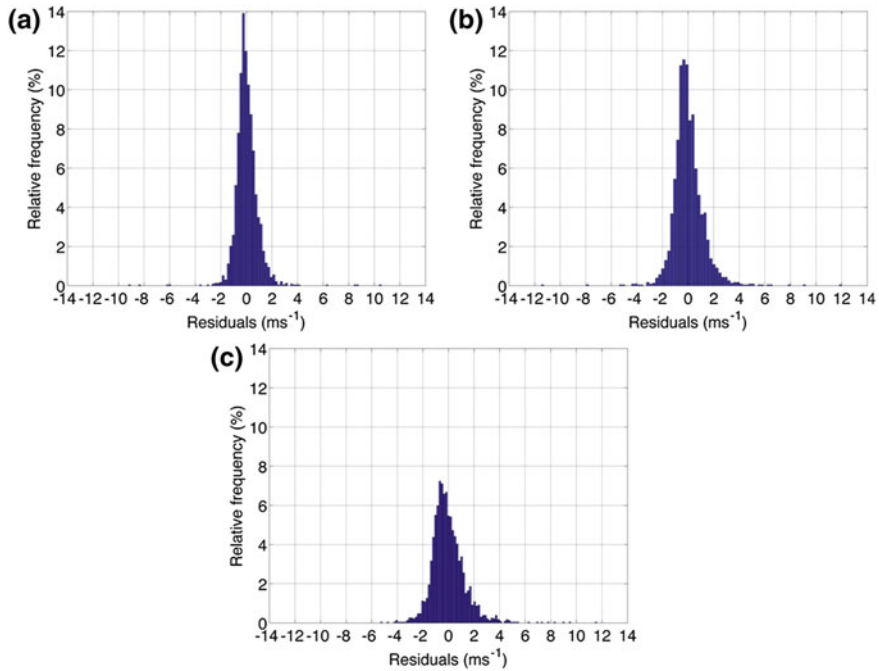


Fig. 12.9 Residuals' distributions for $t + 1$ (a), $t + 2$ (b) and $t + 3$ (c) ANN-based predictions

The higher partial regression coefficients are associated with the wind speed at Platania (0.4064) and at Souda station (0.3782), attributed to the coastal characteristics of the TEI and Platania stations and to the proximity of the TEI and Souda measurement sites.

Regarding the RBF-ANN model and the selection of the optimum spread parameter value, the minima of the MAE error on the validation set is observed after a sharp MAE decrease. In this spread parameter region the neurons do not respond to overlapping regions of the input space. For larger values, the MAE error increases gradually, reaching a secondary maximum and remains constant thereafter as all the neurons respond with the same manner.

The model evaluation statics for the TEI station for both RBF-ANN and MLR approaches are presented in Table 12.4. A general remark is that the nonlinear RBF-ANN model outperforms the linear MLR scheme and that both models perform reasonably well. The explained variance is 73.77 % for the RBF-ANN model and close to 70 % (69.1 %) for the MLR scheme and both scheme exhibit high index of agreement values (0.9213 and 0.8925 respectively) and minimal bias errors.

The comparison of the observed and the predicted wind speed values for both models are presented in Fig. 12.10 scatter plots and the respective residuals'

Table 12.4 Model performance metrics for the TEI station

	R	R ²	MBE (ms ⁻¹)	MAE (ms ⁻¹)	RMSE (ms ⁻¹)	d
MLR	0.8313	0.6910	0.0089	0.7487	1.0760	0.8925
RBF-ANN	0.8589	0.7377	0.0092	0.6944	0.9853	0.9213

Fig. 12.10 Comparison of the predicted and observed wind speed at the TEI station for the RBF-ANN (a) and for the MLR scheme (b)

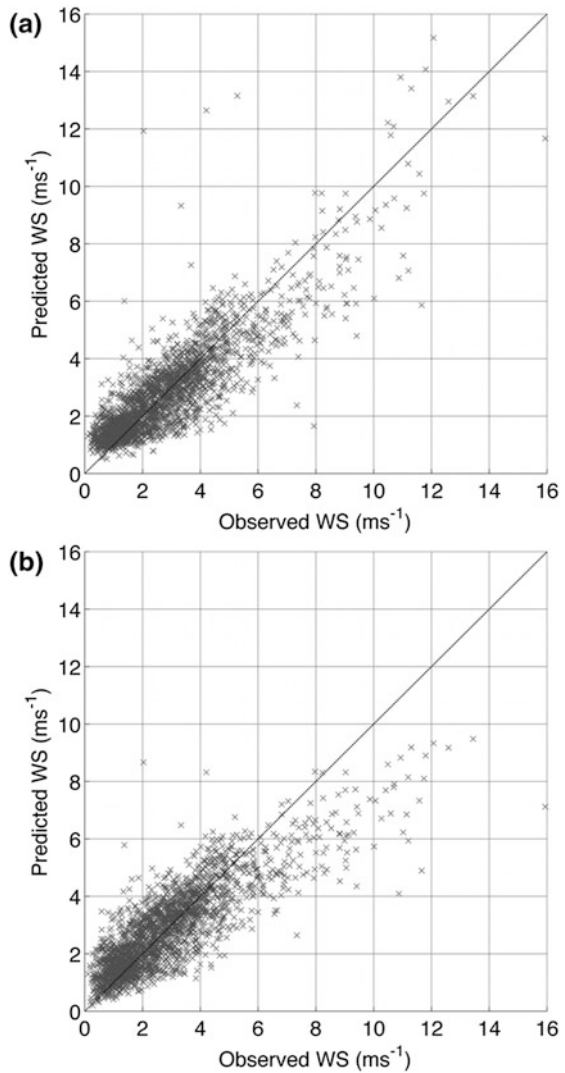
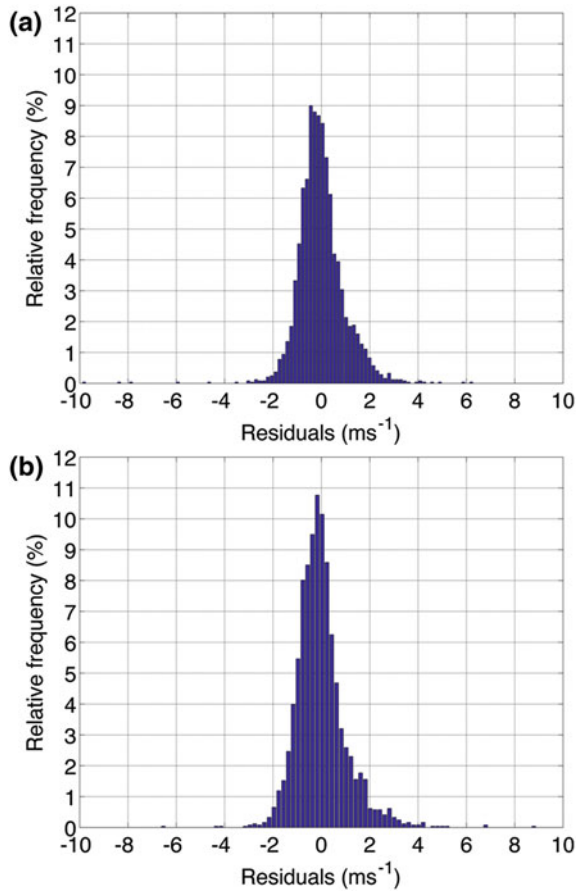


Fig. 12.11 Residuals distribution for the RBF-ANN (a) and the MLR (b) model



distributions are given in Fig. 12.11. Limited data dispersion is observed for both models, while the linear model exhibits signs of under-prediction for the higher wind speed values. In both cases the residuals are symmetrically distributed around 0 ms⁻¹.

Moreover, a time series comparison between the observed and the predicted wind speed from the RBF-ANN model are presented in Fig. 12.12 for the period 21/6/2006–19/7/2006. The predicted wind speed time series follows closely the observed values with no signs of systematic errors. An additional statistical comparison of the observed and the RBF-ANN predicted time series is performed based on their resulting wind speed frequency distributions and the corresponding two-parameter Weibull distribution fits (Fig. 12.13). The two Weibull probability density functions are assessed for statistically significant differences, using the paired *t* test. The null hypothesis that the frequency differences have zero mean is accepted the 0.05 significance level (*p* value = 0.6439).

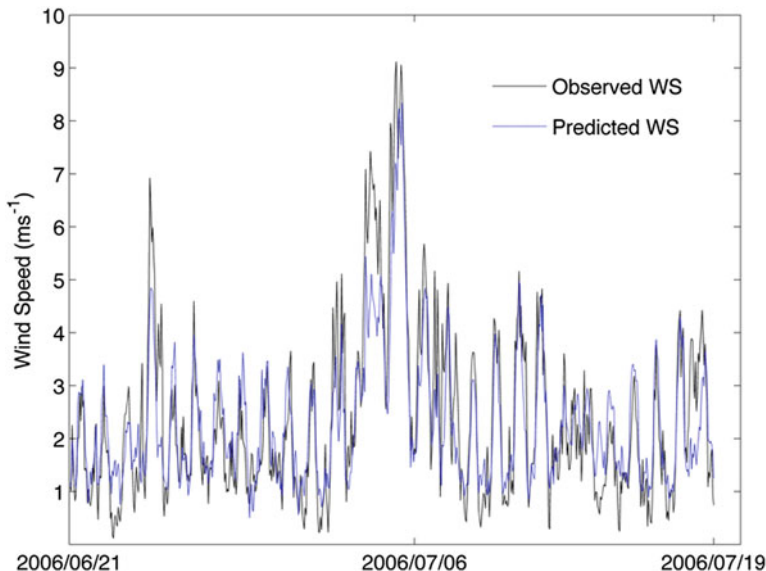
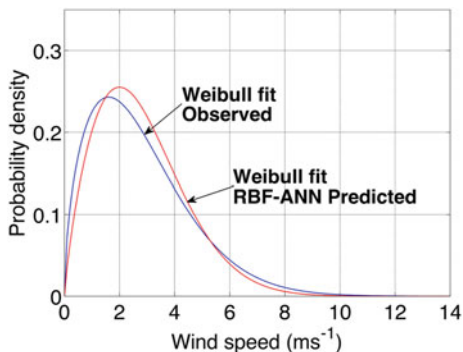


Fig. 12.12 Time series comparison of wind speed between observed and RBF-ANN-based estimation

Fig. 12.13 Weibull probability distributions fits to the observed time series ($k = 1.558$ and $c = 3.102 \text{ ms}^{-1}$) (a) and to the RBF-ANN predicted time series ($k = 1.794$ and $c = 3.148 \text{ ms}^{-1}$)



12.4 Conclusions

The ability of neural networks to spatial estimate and predict short-term wind speed values is studied extensively and is well established. We reviewed the theoretical background, the mathematical formulation, the relative advantages, and limitations of ANN methodologies applicable to the field of wind speed time series and spatial modeling. Then, we have applied ANNs methodologies in the case of a specific region with complex terrain at Chania coastal region, Crete island, Greece. Details of the implementation issues are given along with the set of metrics for evaluating the accuracy of the methodology. A number of alternative feedforward

ANN topologies have been applied in order to assess the spatial and time series wind speed prediction capabilities. For the 1, 2, and 3 h ahead wind speed temporal forecasting at a specific site ANNs were trained based on the current and the five previous wind speed observations from the same site using the Levenberg–Marquardt backpropagation algorithm with the optimum architecture being the one that minimizes the MAE on the validation set. For the spatial estimation of wind speed at a target site the nonlinear RBF-ANN were compared versus the linear MLR scheme, using the concurrent wind speed observations from five sites at the same region. The underlying wind speed temporal and spatial variability is found to be modeled efficiently by the ANNs.

References

- Barbounis TG, Theocharis JB (2007) Locally recurrent neural networks for wind speed prediction using spatial correlation. *Inform Sci* 177(24):5775–5797. doi:[10.1016/j.ins.2007.05.024](https://doi.org/10.1016/j.ins.2007.05.024)
- Beyer H, Degner T, Hausmann J, Hoffmann M, Rujan P (1994) Short term prediction of wind speed and power output of a wind turbine with neural networks. In: *Proceedings of the 5th European wind energy association conference and exhibition*. Thessaloniki, Greece, pp 349–352
- Bilgili M, Sahin B, Yasar A (2007) Application of artificial neural networks for the wind speed prediction of target station using reference stations data. *Renew Energ* 32:2350–2360. doi:[10.1016/j.renene.2006.12.001](https://doi.org/10.1016/j.renene.2006.12.001)
- Bishop CM (1995) *Neural networks for pattern recognition*. Oxford University Press, Cambridge
- Bouzgou H, Benoudjit N (2011) Multiple architecture system for wind speed prediction. *Appl Energ* 88:2463–2471. doi:[10.1016/j.apenergy.2011.01.037](https://doi.org/10.1016/j.apenergy.2011.01.037)
- Cadenas E, Rivera W (2007) Wind speed forecasting in the South coast of Oaxaca, Mexico. *Renew Energ* 32:2116–2128. doi:[10.1016/j.renene.2006.10.005](https://doi.org/10.1016/j.renene.2006.10.005)
- Cellura M, Cirrincione G, Marvuglia A, Miraoui A (2008) Wind speed spatial estimation for energy planning in Sicily: Introduction and statistical analysis. *Renew Energ* 33:1237–1250. doi:[10.1016/j.renene.2007.08.012](https://doi.org/10.1016/j.renene.2007.08.012)
- Costa A, Crespo A, Navarro J, Lizcano G, Madsen H, Feitosa E (2008) A review on the young history of the wind power short-term prediction. *Renew Sust Energ Rev* 12(6):1725–1744. doi:[10.1016/j.rser.2007.01.015](https://doi.org/10.1016/j.rser.2007.01.015)
- Cybenco G (1989) Approximation by superposition of a sigmoidal function. *Math Control Signal* 2:303–314. doi:[10.1007/BF02551274](https://doi.org/10.1007/BF02551274)
- Deligiorgi D, Philippopoulos K (2011) Spatial interpolation methodologies in urban air pollution modeling: application for the greater area of metropolitan Athens, Greece. In: Nejadkoorki F (ed) *Advanced air pollution*, InTech Publishers, doi: [10.5772/17734](https://doi.org/10.5772/17734)
- Deligiorgi D, Kolokotsa D, Papakostas T, Mantou E (2007) Analysis of the wind field at the broader area of Chania, Crete. In: *Proceedings of the 3rd IASME/WSEAS International Conference on Energy, Environment and Sustainable Development*, pp 270–275
- Fadare DA (2010) The application of artificial neural networks to mapping of wind speed profile for energy application in Nigeria. *Appl Energ* 87(3):934–942. doi:[10.1016/j.apenergy.2009.09.005](https://doi.org/10.1016/j.apenergy.2009.09.005)
- Fausett LV (1994) *Fundamentals neural networks: architecture, algorithms, and applications*. Prentice-Hall, Inc., Englewood Cliffs
- Fox DG (1981) Judging air quality model performance. *B Am Meteorol Soc* 62:599–609. doi:[10.1175/1520-0477\(1981\)062<0599:JAQMP>2.0.CO;2](https://doi.org/10.1175/1520-0477(1981)062<0599:JAQMP>2.0.CO;2)

- Gardner MW, Dorling SR (1998) Artificial neural networks (the multilayer perceptron)-A review of applications in the atmospheric sciences. *Atmos Environ* 32:2627–2636. doi:[10.1016/S1352-2310\(97\)00447-0](https://doi.org/10.1016/S1352-2310(97)00447-0)
- Heaton J (2005) Introduction to neural networks with Java. Heaton Research Inc., Chesterfield
- Hornik K, Stinchcombe M, White H (1989) Multilayer feedforward networks are universal approximators. *Neural Netw* 2:359–366. doi:[10.1016/0893-6080\(89\)90020-8](https://doi.org/10.1016/0893-6080(89)90020-8)
- Jain A, Mao J, Mohiuddin KM (1996) Artificial neural networks: a tutorial. *Computer* 29(3): 31–44
- Kalogirou SA (2001) Artificial neural networks in renewable energy systems applications: a review. *Renew Sust Energy Rev* 5:273–401. doi: [10.1016/S1364-0321\(01\)00006-5](https://doi.org/10.1016/S1364-0321(01)00006-5)
- Kamal L, Jafri ZY (1997) Time series models to simulate and forecast hourly averaged wind speed in Quetta, Pakistan. *Sol Energy* 61(1):23–32. doi: [10.1016/S0038-092X\(97\)00037-6](https://doi.org/10.1016/S0038-092X(97)00037-6)
- Kariniotakis G, Stavrakakis GS, Nogaret EF (1996) Wind power forecasting using advanced neural network models. *IEEE T Energy Convers* 11(4):762–7. doi: [10.1109/60.556376](https://doi.org/10.1109/60.556376)
- Koletsis I, Lagouvardos K, Kotroni V, Bartzokas A (2009) The interaction of northern wind flow with the complex topography of Crete island-part 1: observational study. *Nat Hazards Earth Syst Sci* 9:1845–1855. doi: [10.5194/nhess-9-1845-2009](https://doi.org/10.5194/nhess-9-1845-2009)
- Koletsis I, Lagouvardos K, Kotroni V, Bartzokas A (2010) The interaction of northern wind flow with the complex topography of Crete island-part 2: numerical study. *Nat Hazards Earth Syst Sci* 10:1115–1127. doi: [10.5194/nhess-10-1115-2010](https://doi.org/10.5194/nhess-10-1115-2010)
- Kotroni V, Lagouvardos K, Lalas D (2001) The effect of the island of Crete on the etesian winds over the Aegean sea. *Q J R Meteorol Soc* 127:1917–1937. doi: [10.1002/qj.49712757604](https://doi.org/10.1002/qj.49712757604)
- Lei M, Shiyang L, Chuanwen J, Hongling L, Yan Z (2009) A review on the forecasting of wind speed and generated power. *Renew Sust Energy Rev* 13:915–920. doi: [10.1016/j.rser.2008.02.002](https://doi.org/10.1016/j.rser.2008.02.002)
- Li G, Shi J (2010) On comparing three artificial neural networks for wind speed forecasting. *Appl Energy* 87:2313–20. doi: [10.1016/j.apenergy.2009.12.013](https://doi.org/10.1016/j.apenergy.2009.12.013)
- Luo W, Taylor CM, Parker RS (2008) A comparison of spatial interpolation methods to estimate continuous wind speed surfaces using irregularly distributed data from England and Wales. *Int J Climatol* 28:947–959. doi: [10.1002/joc.1583](https://doi.org/10.1002/joc.1583)
- Mohandes M, Rehman S, Halawani TO (1998) A neural networks approach for wind speed prediction. *Renew Energy* 13(3):345–354. doi: [10.1016/S0960-1481\(98\)00001-9](https://doi.org/10.1016/S0960-1481(98)00001-9)
- More A, Deo MC (2003) Forecasting wind with neural networks. *Mar Struct* 16(1):35–49. doi: [10.1016/S0951-8339\(02\)00053-9](https://doi.org/10.1016/S0951-8339(02)00053-9)
- Oztopal A (2006) Artificial neural network approach to spatial estimation of wind velocity. *Energy Convers Manage* 47:395–406. doi: [10.1016/j.enconman.2005.05.009](https://doi.org/10.1016/j.enconman.2005.05.009)
- Philippopoulos K, Deligiorgi D (2012) Application of artificial neural networks for the spatial estimation of wind speed in a coastal region with complex topography. *Renew Energy* 38(1):75–82
- Poggi P, Muselli M, Notton G, Cristofari C, Louche A (2003) Forecasting and simulating wind speed in Corsica by using an autoregressive model. *Energy Convers Manage* 44:3177–3196
- Powell MJD (1987) Radial basis functions for multivariable interpolation: a review. In: Mason JC, Cox MG (eds) *Algorithms for approximation*. Clarendon Press, Oxford
- Rumelhart DE, Hinton GE, Williams RJ (1986) Learning representations by back-propagating errors. *Nature* 323:533–536
- Soman SS, Zareipour H, Malik O, Mandal P (2010) A review of wind power and wind speed forecasting methods with different time horizons. *North American Power Symposium (NAPS)*, doi: [10.1109/NAPS.2010.5619586](https://doi.org/10.1109/NAPS.2010.5619586)
- Torres LJ, Garcia A, De Blas M, De Francisco A (2005) Forecast of hourly average wind speed with ARMA models in Navarre (Spain). *Sol Energy* 79:65–77. doi:[10.1016/j.solener.2004.09.013](https://doi.org/10.1016/j.solener.2004.09.013)
- Velazquez S, Carta AJ, Matias JM (2011) Comparison between ANNs and linear MCP algorithms in the long-term estimation of the cost per kWh produced by a wind turbine at a

- candidate site: a case study in the Canary Islands. *Appl Energ* 88:3869–3881. doi:[10.1016/j.apenergy.2011.05.007](https://doi.org/10.1016/j.apenergy.2011.05.007)
- Willmott CJ (1982) Some comments on the evaluation of model performance. *B Am Meteorol Soc* 63:1309–1313. doi: [10.1175/1520-0477\(1982\)063<1309:SCOTEO>2.0.CO;2](https://doi.org/10.1175/1520-0477(1982)063<1309:SCOTEO>2.0.CO;2)
- Willmott CJ, Matsuura K (2005) Advantages of the mean absolute error (MAE) over the root mean square error (RMSE) in assessing average model performance. *Clim Res* 30:79–82. doi: [10.3354/cr030079](https://doi.org/10.3354/cr030079)
- Willmott CJ, Ackleson SG, Davis RE, Feddema JJ, Klink KM, Legates DR, O'Donnell J, Rowe CM (1985) Statistics for the evaluation and comparison of models. *J Geophys Res* 90:8995–9005. doi: [10.1029/JC090iC05p08995](https://doi.org/10.1029/JC090iC05p08995)
- Yu H, Wilamowski BM (2011) Levenberg–Marquardt training. In: Wilamowski BM, Irwin JD (eds) *Industrial electronics handbook*, 2nd edn. CRC Press, Boca Raton
- Zhang GP, Patuwo E, Hu M (1998) Forecasting with artificial neural networks: the state of the art. *Int J Forecasting* 14(1):35–62. doi: [10.1016/S0169-2070\(97\)00044-7](https://doi.org/10.1016/S0169-2070(97)00044-7)